

## Tropospheric Vertical Transport Over the Tropical Pacific

S. C. Liu<sup>1\*</sup>, S. A. McKeen<sup>1</sup>, E-Y. Hsie<sup>1</sup>, X. Lin<sup>1</sup>, D. R. Blake<sup>2</sup>, F. S. Rowland<sup>2</sup>, A. R. Bandy<sup>3</sup>, and D. C. Thornton<sup>3</sup>, E. V. Browell<sup>4</sup>, R. E. Newell<sup>5</sup>, Scott Smyth<sup>6</sup> and D. D. Davis<sup>6</sup>

1. Aeronomy Lab/NOAA, Boulder, CO

\* Now at School of Earth and Atmospheric Sciences, GIT, Atlanta, GA

2. Dept. of Chemistry, University of California at Irvine, Irvine, CA

3. Dept. of Chemistry, Drexel University, Philadelphia, PA

4. Langley Res. Center/NASA, Hampton VA

5. Earth, Atmosphere, and Planetary Sciences, MIT, Cambridge, MA

6. School of Earth and Atmospheric Sciences, GIT, Atlanta, GA

### Abstract

Observed vertical distributions of trace gases during two Western Pacific Exploratory Missions (PEM-West A and B) were used to study quantitatively the atmospheric vertical transport processes over the tropical troposphere. In particular, the vertical distribution of CH<sub>3</sub>I which was emitted from the ocean and had a well defined atmospheric sink turned out to be extremely useful for a quantitative evaluation of the vertical transport processes. Similarly, the vertical distribution of dimethyl sulfite (DMS) can be used to derive the vertical transport independently. Our study indicated that the prevailing vertical transport from the marine boundary layer to about 10 km over the tropics was remarkably fast: on the order of 5 days. This is consistent but about twice as fast as the vertical transport derived from the vertical distribution of Radon-222 observed over the United States in summer.

The fast vertical transport in the tropics which is presumably due to strong convective activities can have important implications for the entire atmosphere. Large amount of reactive trace species can be transported from the surface to the upper troposphere, even the lower stratosphere, for example, NO<sub>x</sub> from lightning and trace gases and aerosols emitted from biomass burning in the tropics. In addition, the fast vertical transport coupled with an efficient photochemical sink of ozone in the lower troposphere also provides an excellent explanation for the low column ozone density and the extremely low ozone observed in the entire tropical troposphere. We will discuss these and other important implications of such fast vertical transport processes.

## 1. Introduction

It is well known that vertical transport processes such as convections and turbulence play a pivotal role in the atmospheric dynamics and chemistry. Convections redistribute water vapor over the entire troposphere through both transport and hydrometeor formation and fallout. They are very effective at transporting air masses containing trace gases and aerosols from both anthropogenic and natural sources from the boundary layer into the upper troposphere on relatively short time scales. Deep convections also play an important role in the transport of material from the troposphere into the stratosphere in the tropics and, less frequently, at mid latitudes. Ice particles produced in the convective storms and transported into anvils have a major impact on the radiation budget and thermal balance of the earth. In addition, charge generation of thunderstorms and associated current play crucial roles in maintenance of the global electric circuit and production of nitrogen oxides (NO<sub>x</sub>). Finally, chemical and physical processes occurring within various convective clouds alter the population and physical/chemical characteristics of aerosols.

In this paper we take advantage of the observed vertical distributions of trace gases over the tropical Pacific during two Western Pacific Exploratory Missions (PEM-West A and B) to make a quantitative study of the atmospheric vertical transport processes. PEM-West A and B experiments were designed as part of the NASA Global Troposphere Experiment (GTE) to examine the tropospheric chemistry of the Western Pacific region (Hoell et al., 1996; 1997). The primary objective of the missions was to examine the atmospheric chemistry of ozone and ozone precursors in the Western Pacific region and to establish the effect of anthropogenic influences on tropospheric chemistry. In addition, the project investigated the atmospheric chemistry and transport of sulfur species throughout the region. NASA DC-8 was the primary observation platform. Collaborative

observations were carried out by an aircraft from Japan as well as at ground stations from a number of Asian countries. The PEM-West missions were separated into two phases designed to capture the impact of seasonal meteorological dynamics of the region. The first phase, carried out in the fall of 1991 examined the atmospheric chemistry of the region during a period characterized by relatively clean southwesterly flows from the tropical Pacific (Bachmeir et al., 1996). The second phase, in Spring of 1994, focused on the atmospheric chemistry of the region during the period when the flow patterns are reversed and the Western Pacific region receives air masses that have traveled over the Asian continent (Merrill et al., 1997).

Among the trace gases observed during PEM-West, CH<sub>3</sub>I and DMS are most useful for quantifying the vertical transport because they have relatively simple sources and sinks. Both are emitted primarily from the ocean (e.g. Andeae, 1990; Bates et al., 1992; Happell and Wallace, 1996). There is evidence for an oceanic sink for CH<sub>3</sub>I in the cold water at high latitudes under low light conditions (Happell and Wallace, 1996). This is not the concern of this study as our focus is in the tropics. The predominant sink of CH<sub>3</sub>I is photodissociation. This sink gives CH<sub>3</sub>I a lifetime of about 3 days near the surface and 2 days in the upper troposphere under clear sky conditions. For DMS, oxidation by atmospheric OH radicals is the major sink and results in about 1 day lifetime in the boundary layer and 2 days in the upper troposphere under clear sky conditions. Like Radon-222 (lifetime about 5 days), the tracer frequently used to study regional scale vertical transport over the continent (e.g. Liu et al., 1984), the lifetimes of CH<sub>3</sub>I and DMS are ideal for study regional scale vertical transport over the ocean.

Measurement techniques for DMS and CH<sub>3</sub>I were described by Bandy et al. (1993) and Blake et al. (1996), respectively. The accuracy is important to the determination of the vertical transport. In this context, we note that the GC-MS technique used to measure DMS included

independent calibration runs for each individual measurement. Furthermore, the DMS measurement technique has undergone successfully a rigorous airborne intercomparison with other techniques (Gregory et al., 1993) in which the accuracy was established to be about 1 pptv. Because of the extremely low level of CH<sub>3</sub>I, extra effort has been made to establish the accuracy of the measurements by using two different calibration methods. These methods were discussed briefly in Davis et al. (1996) and in detail in a paper in preparation (Chen et al. 1997). They determined the accuracy of the CH<sub>3</sub>I measurements is about 0.05 pptv. As will be seen later the accuracy of DMS and that of CH<sub>3</sub>I are adequate for a meaningful determination of the vertical transport parameter. Moreover, the consistency between the vertical distributions of the two species provides independent confirmation of the vertical transport parameters derived from each species.

Finally, we will show that the distributions of other species such as O<sub>3</sub>, NO<sub>x</sub> and particularly O<sub>3</sub> observed by remote sensing technique give additional support of the vertical transport parameter derived from CH<sub>3</sub>I and DMS. This is significant because the number of data points and spatial coverage of O<sub>3</sub> observations are more than one order of magnitude greater than those of CH<sub>3</sub>I and DMS as O<sub>3</sub> measurements include both in-situ and remote observations and the time resolution is better than 1 second.

## 2. Measurements and Data Analysis

Shown in Figures 1a and 1b are the vertical distributions of CH<sub>3</sub>I observed in and near the tropics (< 20°N) during PEM-West A and B, respectively. The corresponding distributions of DMS are shown in 2a, and 2b. The data are segregated into six 2 km altitude intervals. The horizontal bar covers the range of all the data in the altitude interval; the rectangle denotes data points between lower 25% and upper 75% values; and the vertical bar near the center represents the median value. From hereon

we will refer to the lowest layer as the boundary layer because the predominant measurements in this layer were taken near 300 meters above the sea level. The total number of points in each figure is on the order of 300 for CH<sub>3</sub>I but only about 100 for DMS. The data points are not evenly distributed at each height interval as the flight patterns of DC-8 were designed to favor the upper troposphere (8 km and above) and the boundary layer. Furthermore, during PEM-W B a large number of DMS measurements are below the detection limit which are not included in the figures. Thus, statistically, the data are more meaningful or representative in the upper troposphere and boundary layer than at other altitudes. For this reason, in the following discussions emphasis will be put on the upper troposphere and the boundary layer.

The most remarkable phenomenon in these figures is that, when the profiles are normalized to a common mixing ratio in the boundary layer, the distributions of DMS are qualitatively and even quantitatively consistent with those of CH<sub>3</sub>I in essentially every aspect. In fact, there are more difference between PEM-West A and B distributions for the same species than the difference between the two species. Specifically, both species show a C-shaped profile during PEM-West B while the profiles during PEM-West A are characterized by a relatively large drop from the boundary to the layers above, and very little change above the boundary layer. On the other hand, there is an important difference between DMS and CH<sub>3</sub>I that the relative variability of DMS tends to be smaller than that of CH<sub>3</sub>I. The major reason is that a significant number of measurements of DMS are below the limit of detection (LOD) which is about 1 pptv. In fact, about 60% of the measurements were below LOD in the middle troposphere during PEM-W B. In the upper troposphere, the percentage of measurements below LOD was about 30%. In comparison, none of the CH<sub>3</sub>I measurements was below LOD. Obviously, the effect of data points below LOD on the median value can not be evaluated quantitatively. One can calculate an upper limit and lower limit of the effect by assuming all the measurements below LOD are zero and equal to

LOD, respectively. We have done the calculations of the upper limit effect for the upper troposphere and the boundary layer where we have most of the measurements as discussed above. For PEM-W A the effect is about 30% and 10% reductions in the median values of DMS in the upper troposphere and boundary layer, respectively. The corresponding effects for PEM-W B is about 20% and 5%. Thus inclusion of the effect of LOD tends to make the vertical profiles of DMS to decrease faster than that of CH3I by about 20%. This is consistent with the fact that DMS has a smaller lifetime than CH3I in the lower troposphere as discussed in the introduction.

Since CH3I and DMS are measured by independent methods (Hoell et al. 1996), the consistency between the vertical distributions of the two species strongly supports that the relatively slow decrease of the mixing ratios of CH3I and DMS from the boundary layer to the upper troposphere is the result of fast vertical transport. This notion is also supported by the fact that other relatively short lived trace species observed at low latitudes are also well mixed vertically. These species include O<sub>3</sub>, NO<sub>x</sub>, H<sub>2</sub>O<sub>2</sub>, and some NMHCs. The vertical distributions of O<sub>3</sub> (in-situ measurements) and NO<sub>x</sub> are particularly significant (Figures 3a, 3b, 4a, and 4b). The latter has a very short photochemical lifetime below 5 km (less than 1 day). The fact that a significant level of NO<sub>x</sub> exits below 5 km (Talbot et al. 1996; Gregory et al. 1996; Singh et al., 1996), and recycling of NO<sub>x</sub> through other odd nitrogen species is significantly smaller than the photochemical sink of NO<sub>x</sub>, strongly suggests that transport is needed to support the level of NO<sub>x</sub>. Furthermore, since the mixing ratios of NO<sub>x</sub> and other odd nitrogen species tend to increase with altitude, fast vertical transport is obviously a good candidate of the process that supplies NO<sub>x</sub> below 5 km. The photochemical lifetime of O<sub>3</sub> below 5 km is about 10 days but increases to more than 100 days above 8 km (Davis et al., 1996; Crawford et al., 1997). In fact, there is more photochemical formation of O<sub>3</sub> than destruction in the upper troposphere because of the relative high concentrations of NO<sub>x</sub> (Davis

et al., 1996; Crawford et al., 1997). As a result, the O<sub>3</sub> in the upper troposphere tends to have a flux divergence. Again, this is consistent with an efficient vertical transport from the upper troposphere to the lower troposphere.

We note that there are substantially more observations of O<sub>3</sub> and NO<sub>x</sub> than those of CH3I and DMS because of faster response times of the instruments of the former species. This increases the statistical significance of the latter species. In this regard, the O<sub>3</sub> vertical distributions observed by the remote sensing technique of lidar backscattering and differential absorption (Browell et al., 1996) are particularly valuable. Figures 5a and 5b depict the latitude and height distributions of O<sub>3</sub> observed by this technique during PEM-W A and B, respectively. The remote sensing capability increases the spatial coverage by a whole dimension, i.e. extend from 1-dimension in-situ measurements along the aircraft tracks to the vertical measurements above and below the tracks. By examining the low O<sub>3</sub> areas of Figures 5a and 5b at low latitudes, it can be seen obviously that the low O<sub>3</sub> levels in the middle and upper troposphere are most likely the result of vertical transport of low O<sub>3</sub> from the boundary layer where significant destruction of O<sub>3</sub> occurs. Furthermore, the patterns of O<sub>3</sub> in Figure 5a, 5b are consistent with those of 1a and 1b (also 2a and 2b), respectively. A remarkable similarity in the vertical distributions is that both O<sub>3</sub> and CH3I show a more graduate decrease with altitude during PEM-W A than those PEM-W B. In fact, a clear C-shape (inverse C-shape for O<sub>3</sub>) altitude distribution exists during PEM-W B in CH3I, DMS and remote O<sub>3</sub>, but absent during PEM-W A. As a result, for all three species, the differences between the boundary layer mixing ratios and the upper tropospheric values are smaller in PEM-W B than those of PEM-W A. Given the consistency between the distributions of remote O<sub>3</sub> and those of CH3I at low latitudes, and the large spatial coverage of the former, we believe that the distributions of CH3I in the boundary layer and the upper troposphere are representative of the prevailing atmospheric conditions during the periods the observations were made. In other words, the distributions are

statistically meaningful and thus can be used to derive average vertical transport parameters such as vertical eddy diffusion coefficients.

Since the remote observations of O<sub>3</sub> and companion observations of aerosols reach as high as about 20 km, the data can also be used to examine the altitude extent of the vertical transport. One can see clearly that the effect of fast vertical transport extends above 12 km where the in-situ observations end. In fact, during PEM-W B the lowest O<sub>3</sub> level in the upper troposphere south of 30°N is between 12 and 14 km (Figure 5b), suggesting that extremely effective vertical transport from the boundary layer to the upper troposphere reaches as high as these altitudes. The corresponding altitudes during PEM-W A occurred about 1 to 2 km lower (Figure 5a). In this context, we note that the apparent top of the vertical transport which is indicated by a sharp increase of O<sub>3</sub> mixing ratio near the tropopause is also about 1 km higher in PEM-W B (near 17 km) than that of PEM-W A. This is consistent with the fact that there are considerable more convective activities (and probably more intense) during PEM-W B than PEM-W A (Merrill et al. 1997; Hoell et al., 1997).

Given the consistent features described above, it is tempting to draw a conclusion from the PEM-W B data that because of the C-shape distributions of trace species, the vertical transport from the boundary layer to the upper troposphere due to convective activities over the tropical Pacific has a prevailing altitude range of 12 to 14 km. This would imply that convections maximize at this altitude range and that, over 30 degrees of latitude (many orders of magnitude over the spatial scale of actual convections), the vertical transport by convections needs to be parameterized by advective type of approach rather than mixing method. This turns out to be false as trajectory analysis and a tracer study have shown that the relatively high O<sub>3</sub> mixing ratios and low levels of CH<sub>3</sub>I and DMS between 4 and 10 km are the result of intrusion of continental air masses (Merrill et al., 1997; Crawford et al., 1997). In other words, the

prevailing O<sub>3</sub> distribution in the tropical Pacific marine air should look more like that of PEM-W A than PEM-W B. In this context, we also note that the "top" of the vertical transport described above is an apparent altitude which is strongly influenced by the high stratospheric O<sub>3</sub> mixing ratio. The actual top must lie above the apparent altitude. Furthermore, examination of remote O<sub>3</sub> and aerosols distributions of individual flights reveals that the top is not nearly as smooth or well defined as those shown in the composite plots in Figures 5a and 5b. In the individual flights (not shown) there are significant number of small pockets of relatively low O<sub>3</sub> above the top and vice versa, suggesting vertical transport/exchange of trace species across the top. I.e. the convections do not stop at the top.

Quantitatively, there are various methods to estimate the rate of vertical transport. The most logical approach to simulate the vertical transport is probably to use a 3-dimensional model. This is being carried out in a separate study that emphasizes the technical aspect of simulation and parameterization of convective processes in the tropics (McKeen et al., 1997). Their results demonstrate that indeed the fast vertical transport can be attributed to the high frequency and large altitude extent of the convection in the tropics. Meanwhile, they suggest that on a scale that is substantially greater than the actual convection, the vertical transport can be simulated by mixing processes, e.g. vertical eddy diffusion coefficient.

The areas covered by the observations during both PEM-W A and B are about several thousand kilometers. This is many orders of magnitude greater than the areas under active convective activities along the flight tracks. Under these conditions, a 1-dimensional eddy diffusion approach can provide valuable information about the vertical transport. By fitting a straight line between the median value of the boundary layer and that of the upper troposphere as indicated in Figure 6a, we obtain an eddy diffusion coefficient of 87 m<sup>2</sup>s<sup>-1</sup> for PEM-W A. For PEM-W B (Figure 6b), an eddy diffusion coefficient of 202 m<sup>2</sup>s<sup>-1</sup> is needed because the decrease in the mixing ratio of CH<sub>3</sub>I

between the boundary layer and upper troposphere is about a factor of two smaller than that of PEM-W A. A 50% cloud cover that is consistent with the observation is assumed in the calculation of CH<sub>3</sub>I photolysis rate. CH<sub>3</sub>I instead of DMS is used for the calculation because there are significantly more data points than DMS and no LOD point as discussed earlier. In addition, we have neglected the data between the boundary layer and 10 km because of fewer data points. Obviously this is not a problem for PEM-W A as the eddy diffusion distribution line of CH<sub>3</sub>I with constant  $87 \text{ m}^2\text{s}^{-1}$  eddy diffusion coefficient (Figure 6a) fits the median values quite well over the entire altitude. But this is not the case for PEM-W B as the data points between the boundary layer and 10 km lie significantly below the calculated distribution line (Figure 6b). Moreover, this problem can not be dismissed by arguing that the data points between the boundary layer and 10 km are too few to be representative because, as discussed earlier, the consistency between remote O<sub>3</sub> observations (Figure 5b) and in-situ data (Figure 1b) strongly suggests that the data points between the boundary layer and 10 km are representative of the ambient conditions. Thus, some process(s) other than convective vertical transport must play a significant role in the vertical distributions of trace species during PEM-W B. Indeed, as discussed earlier, a closer examination through trajectory analysis and continental tracers reveals that the majority of the data points between the boundary layer and 10 km at low latitudes during PEM-W B originate from continental areas where little emissions of CH<sub>3</sub>I and DMS is expected. In contrast, few data points at low latitudes during PEM-W A originated from continental areas (Bachmeier et al., 1996).

These eddy diffusion coefficients are very large. For comparison, the eddy diffusion coefficient derived from Rn-222 over the United States was only about  $40 \text{ m}^2\text{s}^{-1}$  under summer conditions, and about  $20 \text{ m}^2\text{s}^{-1}$  for spring/fall conditions (Liu et al., 1984). In terms of transport time, the vertical velocity can be shown to be approximately the eddy coefficient divided by the scale height of the mixing ratio of

CH<sub>3</sub>I. This gives a vertical velocity of about  $1.6 \text{ cm s}^{-1}$  for PEM-W A. Thus it takes only about six days to transport the boundary layer air up to 10 km altitude. This is consistent with an analytical derivation of the vertical transport time that is based on a reasonable assumption that the transport of CH<sub>3</sub>I from the boundary layer to 10 km is in a steady state with the photochemical loss of CH<sub>3</sub>I during the course of the transport. The derivation can be done in the following steps: the average photochemical lifetime of CH<sub>3</sub>I between the boundary layer and 10 km with 50% cloudiness is about 5 days; the mixing ratio of CH<sub>3</sub>I in the boundary layer is about six times of that at 10 km which is about 20% less than two e-folding time; therefore, the transport time from the boundary layer to 10 km should be approximately 20% less than two average photochemical lifetimes of CH<sub>3</sub>I, i.e. eight days. Given the approximate nature of deriving transport time from both methods, we consider the two vertical transport times are in very good agreement with each other. For PEM-W B, the vertical transport time derived analytically is about 5.5 days which is significantly shorter than that during PEM-W A. This is most likely due to the fact that there were considerable more convective activities during PEM-W B than PEM-W A as discussed above.

### 3. Implications and Conclusions

One of the most important manifestations of the fast vertical transport obviously is that short lived species can be transported to the upper troposphere in significant quantities. This can be demonstrated quantitatively by using DMS observed during PEM-W A as an example: with a median boundary layer mixing ratio of about 25 pptv and eddy diffusion coefficient of  $87 \text{ m}^2\text{s}^{-1}$ , one can calculate the vertical flux out of the boundary layer to be  $11 \times 10^8 \text{ cm}^2\text{s}^{-1}$  and the flux reaching 10 km to be  $1.3 \times 10^8 \text{ cm}^2\text{s}^{-1}$ . However, if one assumes a moderate eddy coefficient of  $20 \text{ m}^2\text{s}^{-1}$ , the fluxes out of the boundary layer would decrease modestly to  $5.6 \times 10^8 \text{ cm}^2\text{s}^{-1}$ , but the flux reaching 10 km would decrease to  $0.07 \times 10^8 \text{ cm}^2\text{s}^{-1}$ , a factor of 19 lower. The

corresponding factor for PEM-W B is even greater, about 60! The drastic decrease of the flux reaching 10 km is because the mixing ratio of DMS is an exponential function of its scale height which is proportional to the square root of eddy diffusion coefficient. We note that the scale height is also proportional to the square root of the photochemical loss rate. Therefore, the flux reaching 10 km should change even more drastically for a trace species with lifetime shorter than that of DMS.

Transport of significant quantities of short lived species from the boundary layer to the upper troposphere and even lower stratosphere over the tropics has been suggested to have a significant impact on the regional and/or global photochemistry because of the efficient dispersion effect of strong horizontal winds in those regimes. For example, transport of CH<sub>3</sub>I and other iodine species to the stratosphere in the tropics was proposed to have a significant effect on the photochemistry of the lower stratosphere (Solomon et al., 1995). In addition, Davis et al. (1996) evaluated the photochemistry of iodine species of upper tropospheric during PEM-W A and found a modest impact on the destruction of O<sub>3</sub> and the ratio of HO<sub>2</sub> to OH. Furthermore, in tropical regions strongly affected by pollutants emitted from biomass burning, recent TRACE-A experiment has shown a substantial impact of convective transport of the pollutants on the photochemistry of the upper troposphere (Fishman et al., 1996; Jacob et al., 1996; Pickering et al., 1996).

A potential far reaching implication of the fast vertical transport that has not been considered before is the transport of volatile organic compounds (VOC) and their photochemical products emitted from biogenic sources over the tropical Pacific such as Micronesia and Southeast Asia. By assuming an average overall VOC lifetime of one day, we estimate that 2.5% and 9% of VOC emitted at the surface would be transported above 10 km for eddy diffusion coefficient of 87 m<sup>2</sup>s<sup>-1</sup> and 202 m<sup>2</sup>s<sup>-1</sup>, respectively. If these values are adopted as a range for the entire tropical region,

we can estimate the range of VOC flux reaching 10 km based on the global natural VOC emission distribution derived by Guenther et al. (1995). These authors calculated about 50% or 575 TgC/yr of natural VOC are emitted between 15°N and 15°S. Multiply the 575 TgC/yr by 2.5% and 9%, we get a range of about 15 to 50 TgC/yr of natural VOC reaching 10 km between 15°N and 15°S. VOC fluxes of this range are highly significant to the photochemistry of the upper troposphere, especially in an environment that is expected to have significant amount of NO<sub>x</sub> generated by lightning associated with convections over the continents (Bradshaw et al., 1996; Crawford et al., 1997). For comparison, based on average ambient conditions of PEM-W A and B we estimate the oxidation rates of CH<sub>4</sub> and CO between 10 to 15 km and 15°N and 15°S to be only about 5 and 25 TgC/yr, respectively. Therefore, natural VOC may play a critical role in the photochemistry of the upper troposphere over the tropics and even over the globe. Moreover, the photochemical products of the VOC may also play a major role in the formation, chemistry and optical properties of aerosols and clouds that are extremely important to current issues of tropospheric chemistry and climate (see e.g. IPCC, 1995; Ramanathan et al., 1995)

#### 4. References

- Andeae, M. O., Ocean-atmosphere interactions in the global biogeochemical sulfur cycle, *Mar. Chem.*, 30, 1-29, 1990.
- Bachmeier, Scott A., R. E. Newell, Mark C. Shipham, Yong Zhu, Donald R. Blake, and E. V. Browell, PEM-West A: Meteorological Overview, *J. Geophys. Res.*, 101, 1655-1678, 1996.
- Bandy, A. R., et al., Airborne measurements of sulfur dioxide, dimethyl sulfide, carbon disulfide, and carbonyl sulfide by isotope dilution GC/MS, *J. Geophys. Res.*, 98, 23423-23433, 1993.
- Bates, T. S. B. K. Lamb, A. Guenther, J. Dignon, and R. E. Stoiber, Sulfur emissions to the atmosphere from natural sources, *J. Atm. Chem.*, 14, 315-337, 1992.
- Blake, D. R., et al., Three-dimensional distribution of nonmethane hydrocarbons and halocarbons over the northwestern Pacific during the 1991 PEM-W A, *J. Geophys. Res.*, 101, 1763-1778, 1996.
- Bradshaw, J., S. Smyth, S. C. Liu, D. D. Davis, and R. E. Newell, On the observed distributions of nitrogen oxides in the remote free troposphere, *Review of Geophysics*, in press, 1996.
- Browell, E. V. et al., Large-Scale Air Mass Characteristics Observed Over The Western Pacific During The Summertime, *Journal of Geophysical Research*, 101, 1691-1912, 1996.
- Chen, T., et al., Measurements of iodine compounds, *Journal of Geophysical Research*, submitted, 1997.
- Crawford, J. H., et al., Implications of large scale shifts in tropospheric NO<sub>x</sub> levels in the remote tropical Pacific, *Journal of Geophysical Research*, submitted, 1997.
- Davis, D. D., J. Crawford, S. C. Liu, S. A. McKeen, A. Bandy, D. Thornton, F. S. Rowland, and D. R. Blake, Potential impact of iodine on tropospheric levels of ozone and other critical oxidizing species, *J. Geophys. Res.*, 101, 2135-2147, 1996.
- Fishman, J., et al., NASA GTE TRACE A experiment (September-October 1992): Overview, *J. Geophys. Res.*, 101, 23865-23880, 1996.
- Gregory, G. L., et al., An intercomparison of instrumentation for tropospheric measurements of dimethyl sulfide: Aircraft results for concentrations at ppt level, *Geophys. Res.*, 98, 23373-23388, 1993.
- Gregory, G. L., et al., Chemical signatures of aged Pacific marine air: Mixed layer and free troposphere as measured during PEM-West A, *J. Geophys. Res.*, 101, 1727-1742, 1996.
- Happell, J. D. and D. W. R. Wallace, Methyl iodide in the Greenland/Norwegian Seas and the tropical Atlantic Ocean: Evidence for photochemical production, *Geophys. Res. Lett.*, 23, 2105-2108, 1996.
- Hoell, Jr., J. M. et al., The Pacific Exploratory Mission-West (PEM-West A): September-October 1991, *Journal of Geophysical Research*, 101, 1641-1654, 1996.
- Hoell, Jr., J. M. et al., The Pacific Exploratory Mission-West B(PEM-West B): Feb-March 1994, *Journal of Geophysical Research*, submitted, 1996.
- IPCC, Climate Change, The Science of Climate Change, Edited by J. T. Houghton et al., Published by the Intergovernmental Panel on Climate Change, University Press, Cambridge, 1995.
- Jacob, D. J., et al., Origin of ozone and NO<sub>x</sub> in the tropical troposphere: A photochemical analysis of aircraft observations over the south Atlantic basin, 101, 24235-24250, 1996.
- Liu, S. C., J. R. McAfee, and R. J. Cicerone, Radon 222 and Tropospheric Vertical Transport, *J. Geophys. Res.*, 89, 7291, 1984.
- McKeen, S. A., S.C. Liu, E.-Y. Hsie, D. Blake, T. Chen, D. Thornton, The convective transport of tracers in the tropical marine troposphere during PEM-West B: A three-dimensional model study, *Journal of Geophysical Research*, in press, 1997.
- Merrill, J. T. et al. : A Meteorological Overview for the Pacific Exploratory Mission-West, Phase B, *Journal of Geophysical Research*, in press, 1997.
- Pickering, K. E., et al., Convective transport of biomass burning emissions over Brazil during TRACE A, 101, 23993-24012, 1996.



Ramanathan, V., et al., Warm pool heat budget and shortwave cloud forcing: A missing physics?, *Science*, 267, 499-502, 1995. Singh, H. et al., Reactive Nitrogen and Ozone Over The Western Pacific: Distribution, Partitioning and Sources, *Journal of Geophysical Research*, 101, 1793-1808, 1996.

Solomon, S., et al., On the role of iodine in ozone depletion, *J. Geophys. Res.*, 99, 20491-20499, 1995.

Talbot R. W., et al., Chemical characteristics of continental outflow from Asia to the troposphere over the western Pacific ocean during September-October 1991: Results from PEM-West A, *J. Geophys. Res.*, 101, 1713-1726, 1996.

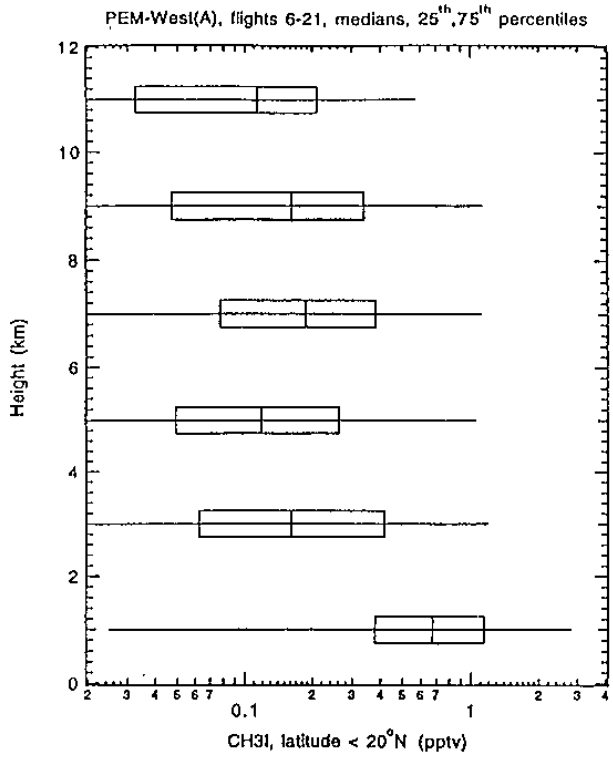


Figure 1a

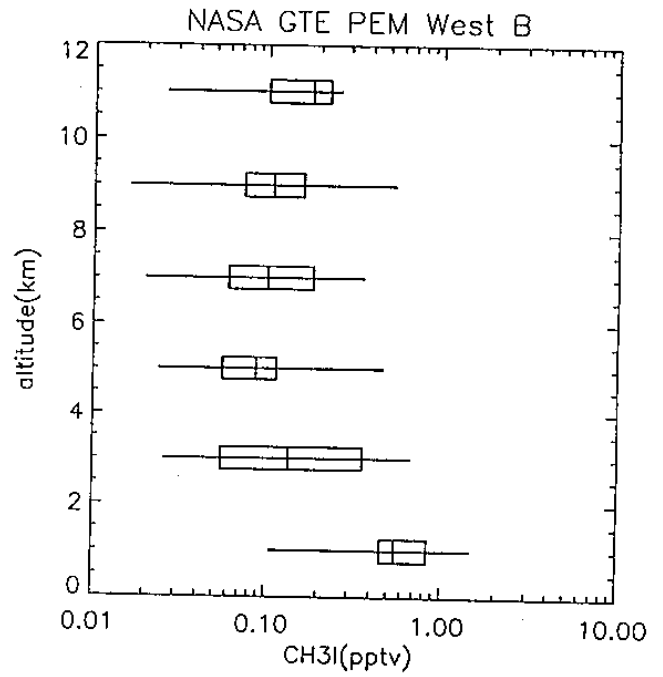


Figure 1b

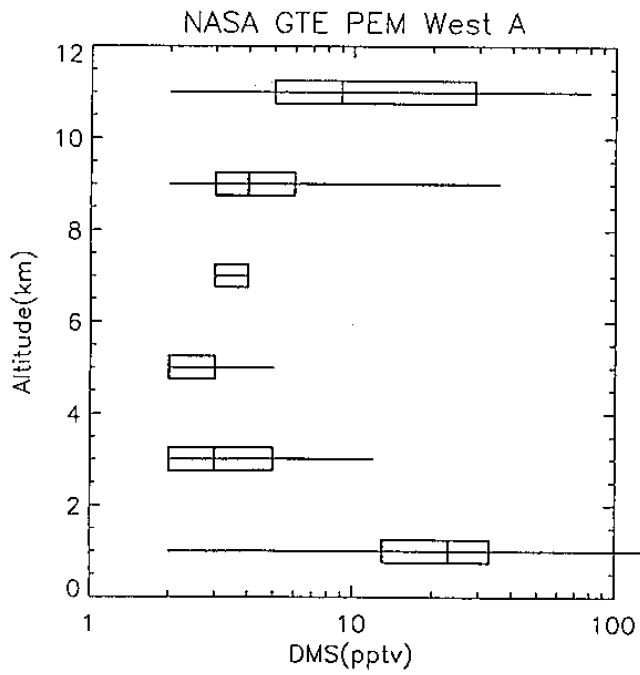


Figure 2a

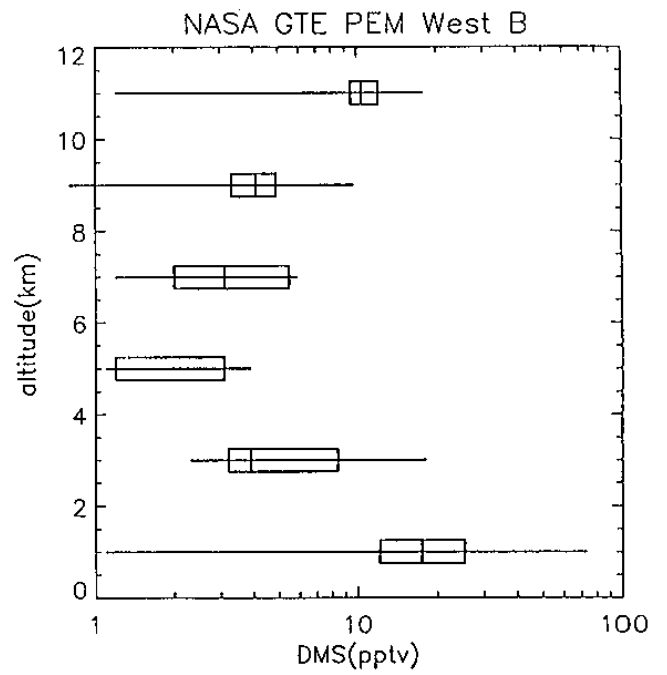


Figure 2b

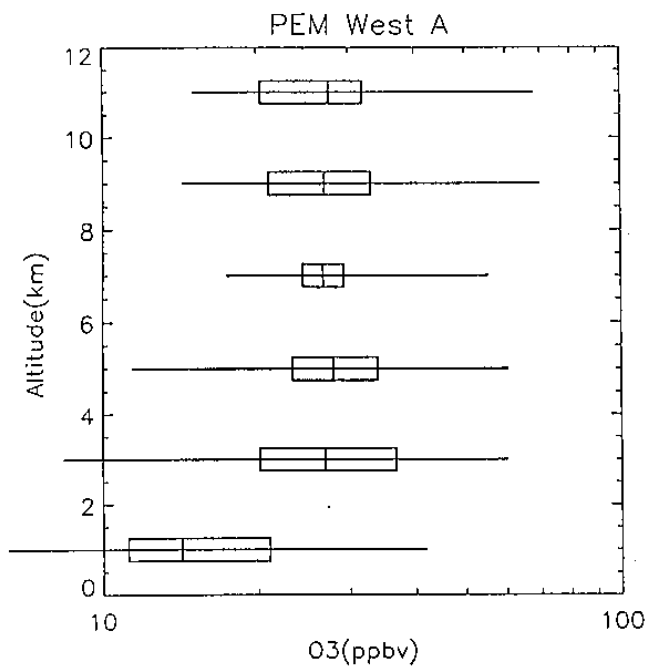


Figure 3a

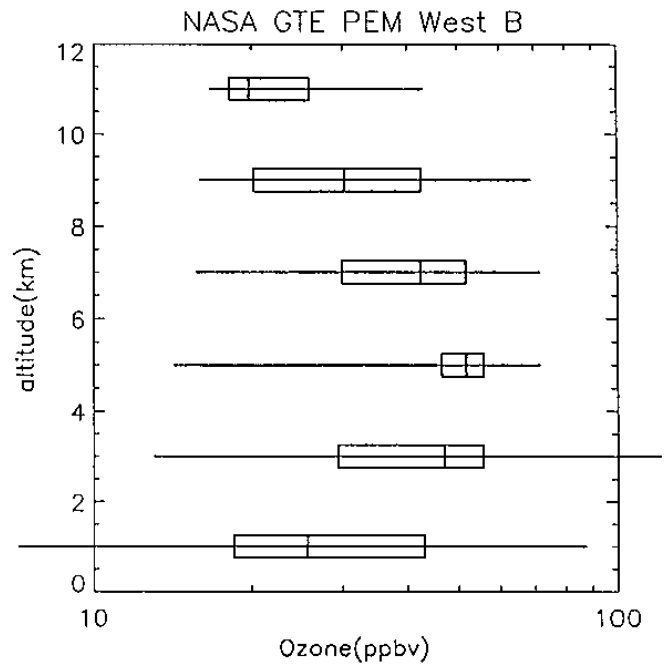


Figure 3b

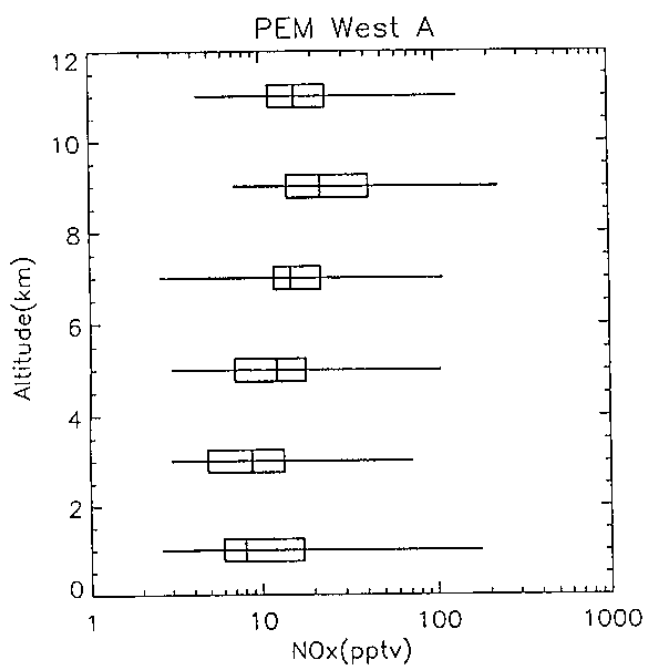


Figure 4a

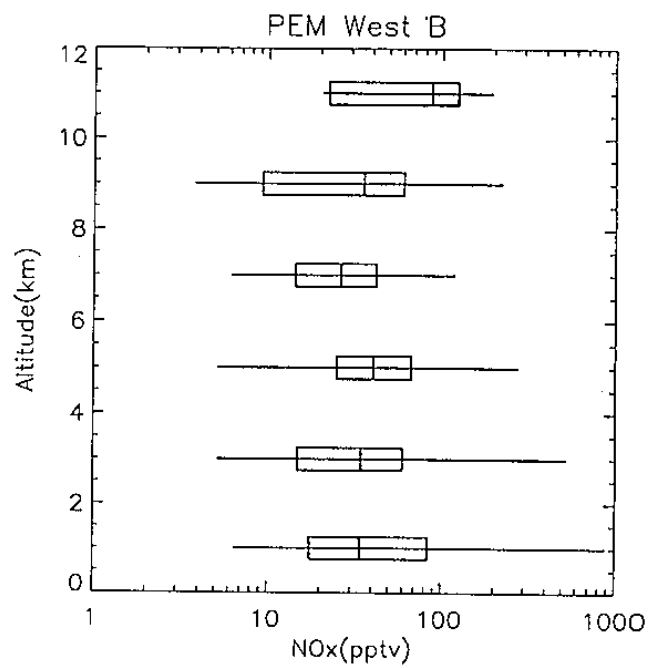
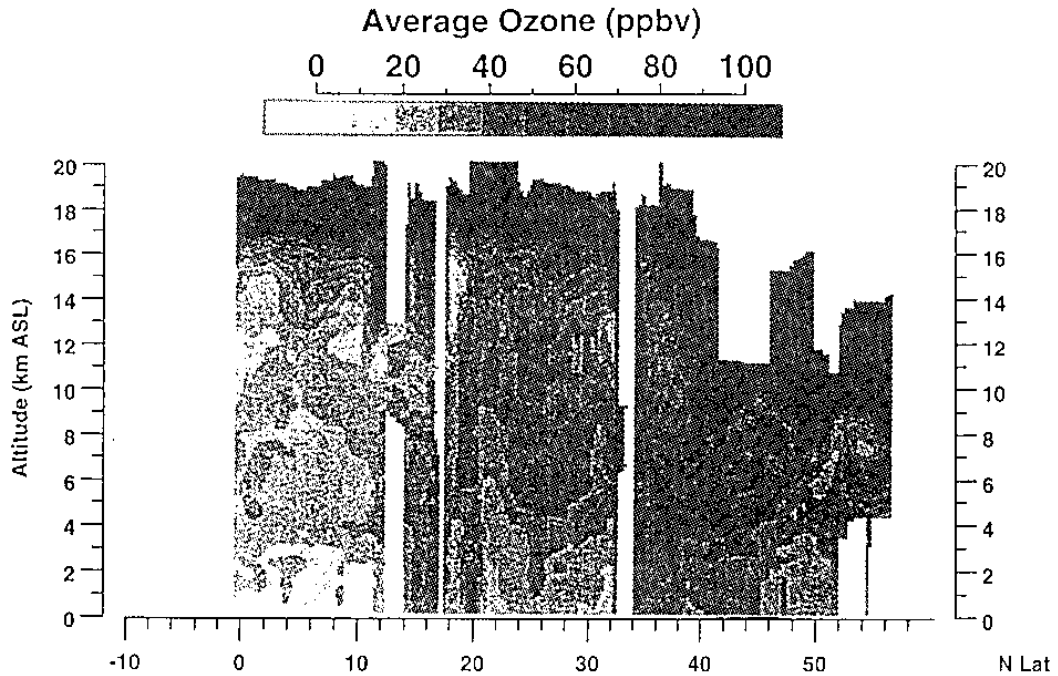


Figure 4b

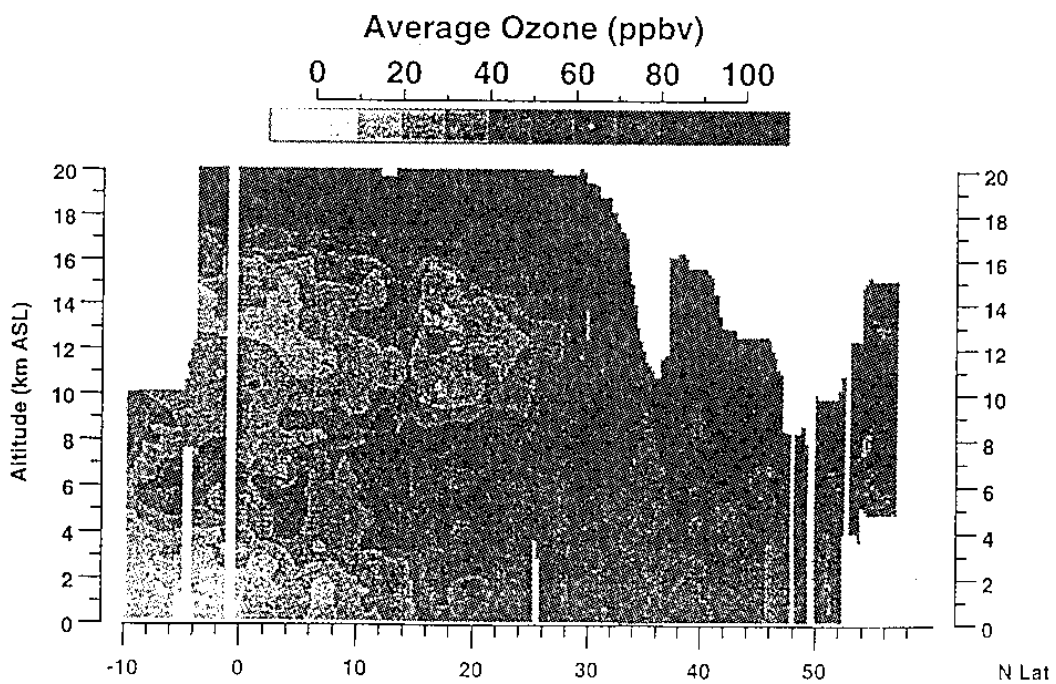
PEMWEST-A  
Latitudinal Ozone Distribution Over  
Western Pacific

Figure 5a



PEMWEST-B  
Latitudinal Ozone Distribution Over  
Western Pacific

Figure 5b



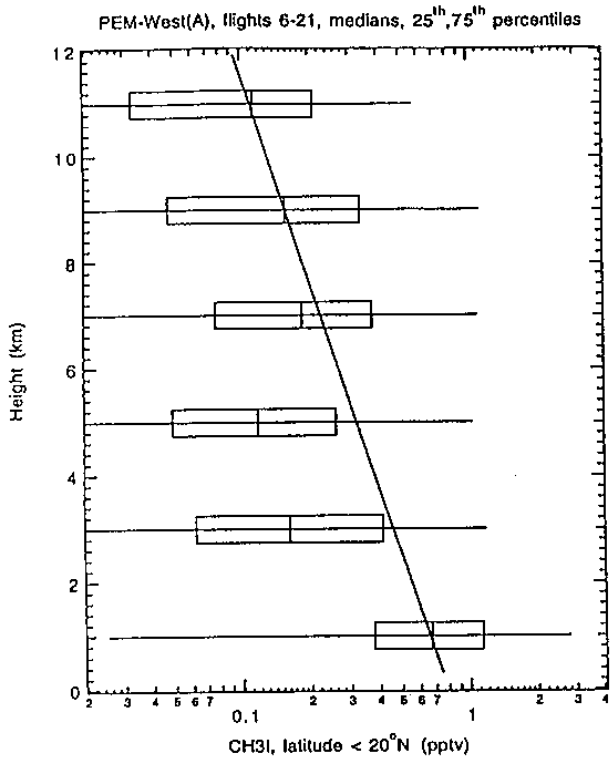


Figure 6a

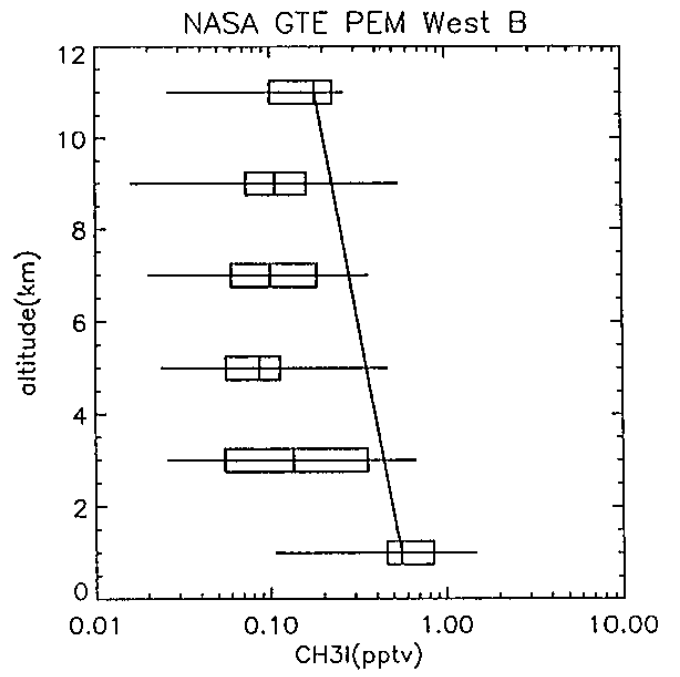


Figure 6b